Weighing the Arches cluster

Christoph Olczak

ARI & MPIA, Heidelberg

NAOC, Beijing

Collaborators:

Andrea Stolte (Argelader Institut für Astronomie, Bonn)

Rainer Spurzem (ARI Heidelberg; NAOC, KIAA Beijing)

The star formation process: characteristic imprints

Characteristics of the star formation process are imprinted in the **IMF** and the **ICMF**.

→ Do we find evidence for environmental dependence?

initial (stellar) mass function (**IMF**)

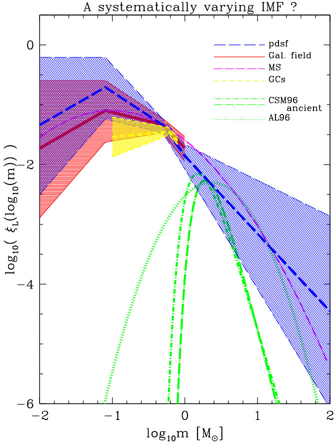

Kroupa (2001)

initial cluster mass function (**ICMF**)

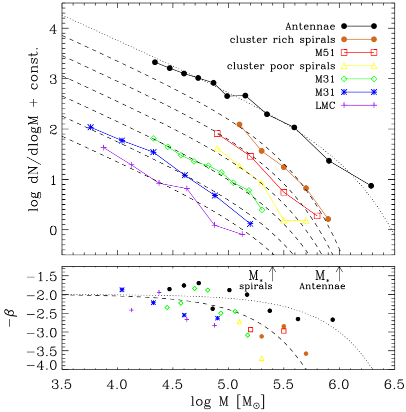

Portegies Zwart et al. (2010)

The Arches cluster

Ideal probes of the variation of the **IMF** and **ICMF**: Galactic “starburst” clusters.
→ Extreme environment: Galactic center.

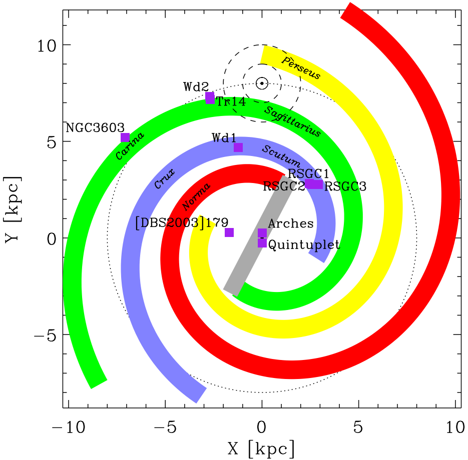

Portegies Zwart et al. (2010)

The Arches Cluster is one of the densest and most massive young Galactic star clusters:

- age: $t \approx 2.5\,\mathrm{Myr}$
- O-stars: $N \approx 150$ $(m_* > 20\,\mathrm{M}_\odot)$
- mass: $M \gtrsim 10^4\,\mathrm{M}_\odot$ $(\rho \gtrsim 10^5\,\mathrm{M}_\odot\,\mathrm{pc}^{-3})$

A top-heavy mass function?

Two independent best mass estimates:

- **photometric**: Espinoza et al. (2009)
  $M(R < 0.4\,\mathrm{pc}) = (3.1 \pm 0.6) \times 10^4\,\mathrm{M}_\odot$
- **kinematic**: Clarkson et al. (2012)
  $M(R < 0.4\,\mathrm{pc}) = (0.90^{+0.40}_{-0.35}) \times 10^4\,\mathrm{M}_\odot$

Measuring the dynamical mass: an observational challenge

Clarkson et al. (2012): "The first kinematic mass measurement of the Arches cluster".
→ Note potential bias due to limited sampling.

1. space

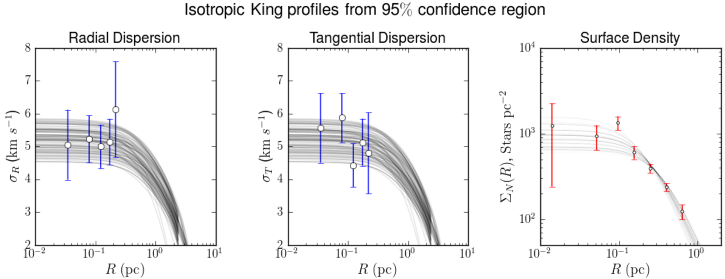

2. mass

observations			models	
K' (mag)	N	σ (km s^{-1})	m (M$_\odot$)	N
10 - 14	67	5.06 ± 0.66	120.0 - 28.0	60 ± 7
14 - 16	72	5.80 ± 0.70	28.0 - 11.0	133 ± 13
16 - 18	107	7.14 ± 1.14	11.0 - 4.0	451 ± 25

Numerical evolution of dynamical models

Models based on parameters estimated by Harfst et al. (2010) and evolved with NBODY6GPU (Aarseth, 2003; Nitadori & Aarseth, 2012).

Using grid of numerical models to fit photometric data:

- single stars
- King-type phase-space distribution (King, 1966)
- **'standard' IMF** with full mass range $0.1 - 150\,\mathrm{M}_\odot$ (Kroupa, 2001)
- **rotation**
- stellar evolution

Two best-fitting (rotating) King models with $W_0 = 3$:

1. **non-rotating** $\mathcal{M}_\mathcal{N}$: $\omega_0 = 0.0,\ N_0 = 65k$ $\quad M_0 = (4.26 \pm 0.06) \times 10^4\,\mathrm{M}_\odot$
2. **rotating** $\mathcal{M}_\mathcal{R}$: $\omega_0 = 1.5,\ N_0 = 59k$ $\quad M_0 = (3.86 \pm 0.07) \times 10^4\,\mathrm{M}_\odot$
   → Note: maximum ω_0 for stable rotation.

Rapid mass segregation in starburst clusters

Energy equipartition drives strong mass segregation of the 100 most massive stars.

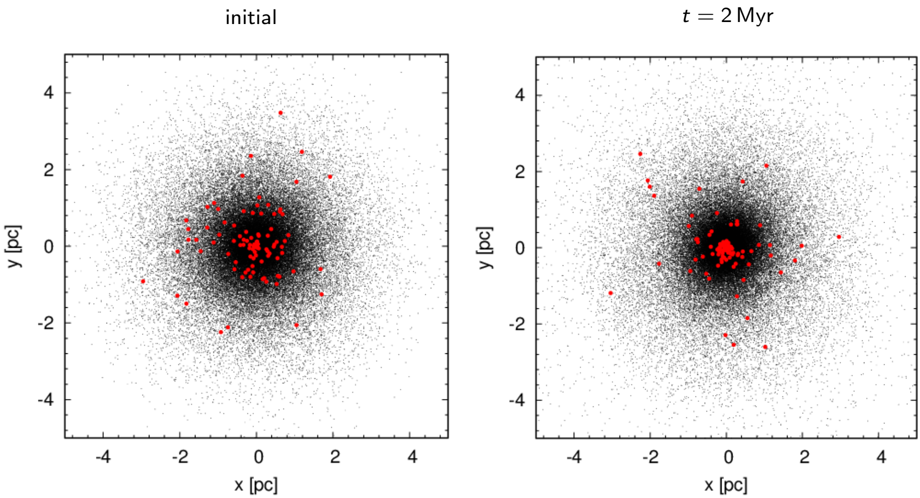

Rapid mass segregation in starburst clusters

Energy equipartition drives strong mass segregation of the 100 most massive stars.

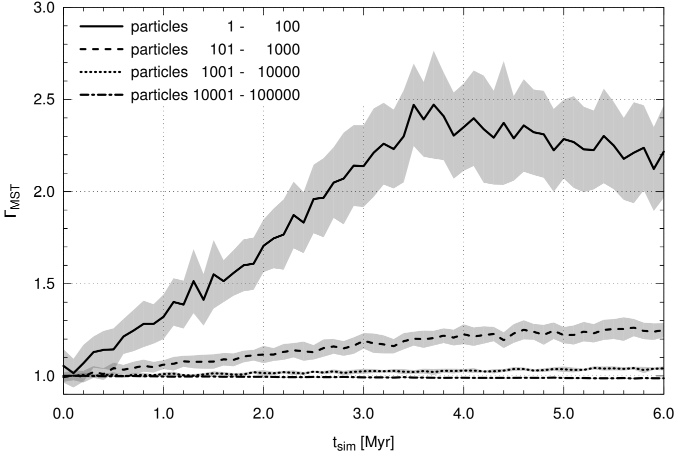

- Mass segregation measure Γ_{MST} from Olczak et al. (2011).

Evolution of the projected velocity dispersion

Comparison of numerical models and observational kinematic data of Clarkson et al. (2012):

- Velocity dispersion as a function of mass and radius projected along the principal axes.

  Note: Black frame indicates observed parameter space.

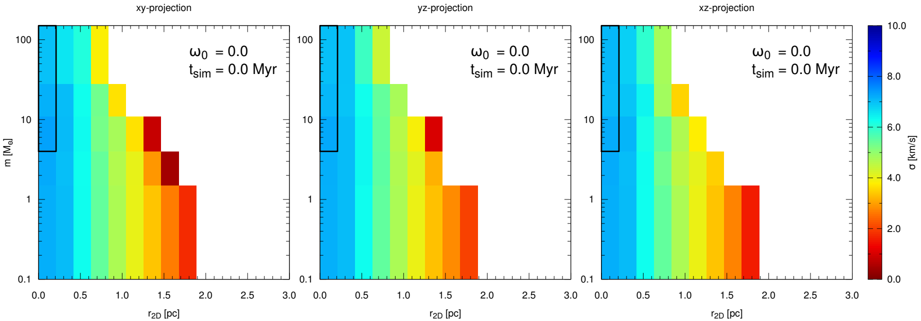

Evolution of the projected velocity dispersion

Comparison of numerical models and observational kinematic data of Clarkson et al. (2012):

- Velocity dispersion as a function of mass and radius projected along the principal axes.

  Note: Black frame indicates observed parameter space.

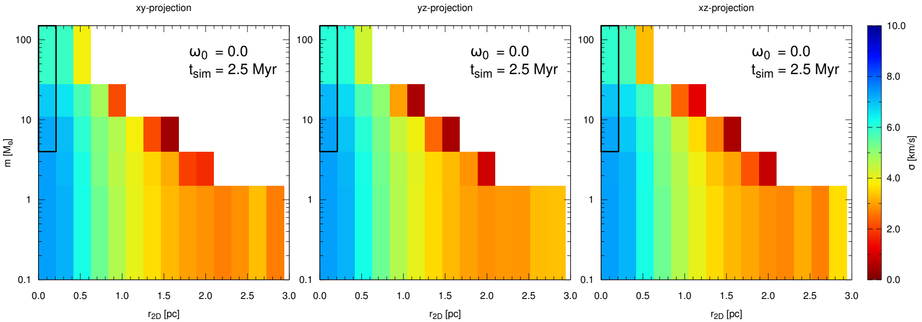

Evolution of the projected velocity dispersion

Comparison of numerical models and observational kinematic data of Clarkson et al. (2012):

- Velocity dispersion as a function of mass and radius projected along the principal axes.

Note: Black frame indicates observed parameter space.

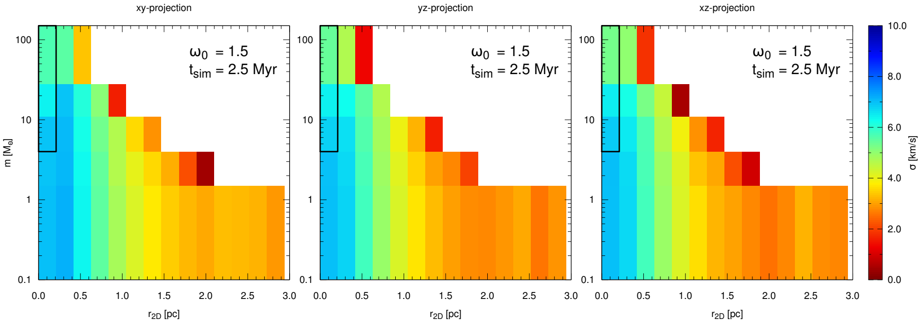

The final comparison of observations and simulations

Good agreement of models and observational data of the Arches cluster suggests:

- $\mathbf{M_0} = \mathbf{4} \times \mathbf{10^4}\ \mathrm{M}_\odot$ ($\approx M_{\rm cl}$!)
- **'standard' IMF** (e.g. Kroupa, 2001)
- **rapid rotation** (with $i \approx 45 - 90^\circ$) → Hénault-Brunet et al. (2012a) + globular clusters

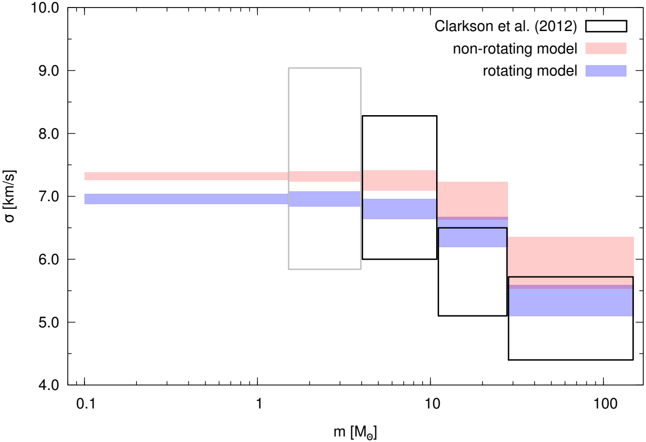

And there are more rotating candidates...

- Hénault-Brunet et al. (2012a): "Evidence for rotation of the young massive cluster R136"

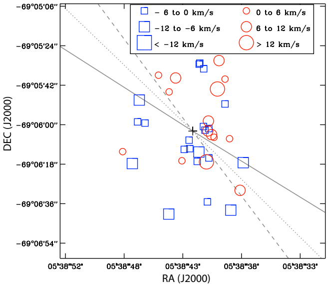

- Gennaro et al. (2011): "Mass segregation and elongation of the starburst cluster Westerlund 1"

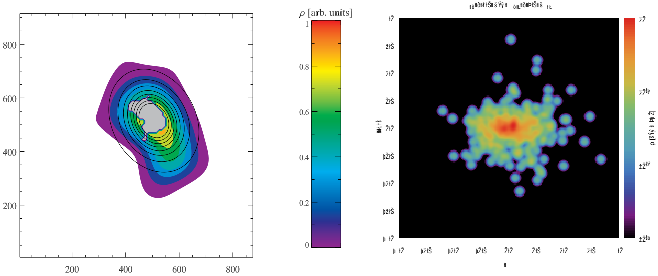

Summary

Initial mass function (IMF)

Despite extreme environmental conditions: observational *photometric* and *kinematic* data of the Arches cluster are consistent with the 'standard' IMF of Kroupa (2001).

▶ No evidence for a non-universal IMF.

Mass segregation

Mass segregation in the Arches cluster evolves very rapidly ($\lesssim 1\,\mathrm{Myr}$).

▶ Observations of starburst clusters are potentially strongly biased by high-mass stars.

Rotation

Our numerical results suggest a rapid rotation of the Arches cluster.

▶ Aequivalent scenario proposed for R136 by Hénault-Brunet et al. (2012b).

Is rapid rotation a common feature of young (massive) star clusters?

A numerical model of the Arches cluster

- Dynamical model (cf. Harfst et al., 2010): gas-free, virial equilibrium, no primordial binaries.
- Five present-day coordinates (Nagata et al., 1995; Figer et al., 2002; Stolte et al., 2008):

$$\vec{r}_{\text{cluster}} = (-24, -100, 10)\,\text{pc}\,, \qquad \vec{v}_{\text{cluster}} = (-190, 95, 0)\,\text{km}\,\text{s}^{-1}$$

- Galactic potential: $M_{\text{gal}}(r) = 4.25 \cdot 10^6 (r[\text{pc}])^{1.2}\,\text{M}_\odot$ (Portegies Zwart et al., 2002).

Best-fitting model with five initial parameters ($N = 74153$):

- mass function slope $\alpha \sim$ IMF of Kroupa (2001)
- lower mass limit $m_{\text{low}} = 0.1\,\text{M}_\odot$ (not well constrained)
- number of massive stars $N_{\text{MS}} = 150$ ($m > 20\,\text{M}_\odot$)
- virial radius $R_{\text{vir}} = 0.7\,\text{pc}$
- King parameter $W_0 = 3$

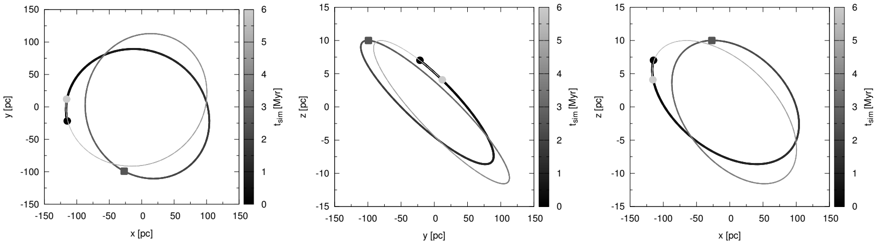

Supplementary data.

Table: Present-day kinematic parameters of the Arches cluster from observations and numerical modeling.
The stellar numbers and velocity dispersions refer to the cluster volume within a projected radius $R \leq 0.2$ pc.

observations			model $\mathcal{M}_\mathcal{N}$		model $\mathcal{M}_\mathcal{R}$		
K' (mag)	N	σ ($\mathrm{km\,s^{-1}}$)	N	σ ($\mathrm{km\,s^{-1}}$)	N	σ ($\mathrm{km\,s^{-1}}$)	m ($\mathrm{M_\odot}$)
10 - 14	67	5.06 ± 0.66	60 ± 7	5.94 ± 0.41	59 ± 8	5.34 ± 0.25	150.0 - 28.0
14 - 16	72	5.80 ± 0.70	133 ± 13	6.93 ± 0.30	123 ± 15	6.43 ± 0.24	28.0 - 11.0
16 - 18	107	7.14 ± 1.14	451 ± 25	7.25 ± 0.16	426 ± 26	6.80 ± 0.16	11.0 - 4.0
18 - 20	97	7.44 ± 1.60	1519 ± 42	7.32 ± 0.08	1442 ± 37	6.96 ± 0.12	4.0 - 1.5
—	—	—	28701 ± 560	7.32 ± 0.06	26997 ± 491	6.96 ± 0.08	1.5 - 0.1

Table: Properties of the evolved models $\mathcal{M}_\mathcal{N}$ and $\mathcal{M}_\mathcal{R}$ compared to published observational estimates.
Note that the z-axis is the rotation axis, hence rotation takes place in the xy-plane.

model	projection	$R < 0.4$ pc					$R < 0.7$ pc	
			$m > 10\,\mathrm{M_\odot}$		$m > 20\,\mathrm{M_\odot}$		$m > 20\,\mathrm{M_\odot}$	
		M ($10^4\,\mathrm{M_\odot}$)	M ($10^3\,\mathrm{M_\odot}$)	N	M ($10^3\,\mathrm{M_\odot}$)	N	M ($10^3\,\mathrm{M_\odot}$)	N
$\mathcal{M}_\mathcal{N}$	xy	1.91 ± 0.03	6.06 ± 0.41	209 ± 12	4.54 ± 0.42	98 ± 7	5.45 ± 0.49	123 ± 10
	xz	1.90 ± 0.03	6.05 ± 0.34	205 ± 14	4.56 ± 0.33	97 ± 7	5.46 ± 0.48	123 ± 10
	yz	1.90 ± 0.03	6.00 ± 0.39	203 ± 17	4.53 ± 0.35	96 ± 8	5.43 ± 0.50	122 ± 10
$\mathcal{M}_\mathcal{R}$	xy	1.58 ± 0.05	5.26 ± 0.49	169 ± 15	4.10 ± 0.50	85 ± 8	5.16 ± 0.60	116 ± 11
	xz	1.90 ± 0.05	6.09 ± 0.59	206 ± 19	4.61 ± 0.58	99 ± 10	5.28 ± 0.59	120 ± 11
	yz	1.89 ± 0.04	6.00 ± 0.57	202 ± 15	4.56 ± 0.55	97 ± 10	5.22 ± 0.59	118 ± 11
Harfst et al. (2010)		—	6.1 ± 1.0	—	—	—	—	—

Aarseth, S. 2003, Gravitational N-body Simulations (Cambridge, Cambridge University Press, 2003, 430 p.)

Clarkson, W. I., Ghez, A. M., Morris, M. R., et al. 2012, ApJ, 751, 132

Espinoza, P., Selman, F. J., & Melnick, J. 2009, A&A, 501, 563

Figer, D. F., Najarro, F., Gilmore, D., et al. 2002, ApJ, 581, 258

Gennaro, M., Brandner, W., Stolte, A., & Henning, T. 2011, MNRAS, 412, 2469

Harfst, S., Portegies Zwart, S., & Stolte, A. 2010, MNRAS, 409, 628

Hénault-Brunet, V., Gieles, M., Evans, C. J., et al. 2012a, A&A, 545, L1

Hénault-Brunet, V., Gieles, M., Evans, C. J., et al. 2012b, ArXiv e-prints

King, I. R. 1966, AJ, 71, 64

Kroupa, P. 2001, MNRAS, 322, 231

Nagata, T., Woodward, C. E., Shure, M., & Kobayashi, N. 1995, AJ, 109, 1676

Nitadori, K. & Aarseth, S. J. 2012, MNRAS, 424, 545

Olczak, C., Spurzem, R., & Henning, T. 2011, A&A, 532, A119

Portegies Zwart, S. F., Makino, J., McMillan, S. L. W., & Hut, P. 2002, ApJ, 565, 265

Portegies Zwart, S. F., McMillan, S. L. W., & Gieles, M. 2010, ARA&A, 48, 431

Stolte, A., Ghez, A. M., Morris, M., et al. 2008, ApJ, 675, 1278